Nonconservative charged-particle swarms in ac electric fields

R. D. White,[1] R. E. Robson,[1] and K. F. Ness[2]
[1]*School of Computer Science, Mathematics and Physics, James Cook University, Cairns QLD 4870, Australia*
[2]*School of Computer Science, Mathematics and Physics, James Cook University, Townsville QLD 4811, Australia*
(Received 24 June 1999)

A time-dependent multiterm technique has been developed and employed to solve the space- and time-dependent Boltzmann equation for charged-particle swarms in ac electric fields. This technique allows for the accurate calculation of both the full set of transport coefficients and the phase-space distribution function. This technique avoids restrictions on the field amplitude and frequency and/or the charged-particle to neutral molecule mass ratio traditionally associated with many contemporary investigations. To our knowledge, it represents the first rigorous treatment of the explicit effects of nonconservative processes on transport coefficients in ac electric fields. The phenomena associated with these explicit effects of nonconservative processes are striking (e.g., negative phase lags in the drift velocity for an attaching gas), and the errors associated with traditional treatments of ionization and attachment on the transport coefficients are highlighted.
[S1063-651X(99)05512-9]

PACS number(s): 51.10.+y, 52.25.Fi, 52.25.Jm, 52.80.Pi

I. INTRODUCTION

Future generation plasma discharge technologies require an accurate knowledge of the transport properties of charged particles (and other constituents) in gases under the influence of space and time varying electric and magnetic fields throughout the entire discharge [1]. In the bulk of a weakly ionized ac plasma discharge, however, far away from the influence of the electrodes, the electric field, though still periodic in time, is approximately spatially homogeneous, and one may consider the boundary free problem often referred to as the swarm problem [2]. Much research has been invested in this problem dating back to the pioneering works of Holstein [3], Margeneau and Hartman [4], and McDonald and Brown [5]. Considerable contributions have also been made by Winkler and co-workers [6,7], Makabe and coworkers [2,8–10], Ferreira and Loureiro [11,12] and others [13] under conditions of spatially homogeneous number density. More recently, interest has centered on the calculation of transport coefficients in ac electric fields in the presence of spatial gradients in the number density, lead by investigations at Keio University [10], the University of Belgrade [14,40,41] and James Cook University [15–18]. These works have unearthed a variety of new phenomena, the most important of which is ''anomalous anisotropic diffusion.'' Reviews of this phenomena can be found in Refs. [10,16–18]. Of particular note is the recent study involving an additional time-dependent magnetic field [40]. However, despite the pivotal role of nonconservative processes in these discharges, e.g., attachment and electron impact ionization, to the present there has been no systematic study of the influence of these processes on the transport coefficients per se in the bulk plasma under the influence of an ac electric field. In a previous paper [18] we briefly reported preliminary investigations highlighting the magnitude of errors associated with neglecting the explicit effect of nonconservative processes on the transport coefficients. These results were verified by the benchmark Monte Carlo simulations performed by the group at the University of Belgrade [41]. It is the primary aim of this paper to present the first systematic study of nonconservative processes in gases in ac electric fields. We highlight the necessary ingredients for the accurate calculation of the transport coefficients up to diffusion in the presence of nonconservative processes, and emphasize the physical implications which arise from their explicit inclusion.

Care must be taken when nonconservative processes are operative to ensure the calculated quantities are what are measured or measurable [19]. In this context, it is the ''bulk'' and not the ''flux'' transport coefficients upon which we focus attention. Generally speaking, this distinction has been ignored in all previous work in the plasma modeling community, and even those in the swarm physics field in some cases. At this point we wish to especially to sound a warning to plasma fluid modelers who implement swarm data, to be aware of the differences in the two sets of transport coefficients (bulk and flux), and to ensure the swarm data are employed correctly. We defer a full discussion of this to a future publication [42]. In this paper we present the required theoretical treatment of the nonconservative corrections, and highlight differences in origin and magnitudes of the bulk and flux transport coefficients in ac electric fields.

The philosophy of our approach is that we build, where possible, upon the extensive experience gained over the decades from the dc theory. The aim is to overcome the restrictions which have in the past plagued ac field studies, particularly the following.

(i) We present a multiterm technique whereby the number of spherical harmonics employed is incremented until the specified accuracy criterion is satisfied. Assumptions of quasi-isotropy of the velocity of the distribution function [3–6,11,13,20], avoiding the ''two-term'' spherical harmonic approximation.

(ii) We retain the temporal dependence of all components of the spherical harmonic expansion i.e., we avoid the restrictions associated with quasistationary approximations [3,6,20], effective field approximations [3,5,11], and low-order Fourier series approximations [4,8,12].

(iii) We make no assumptions about the ratio of the

charged particle to the neutral particle. The code is equally valid for electron and ion swarms.

In this paper, like all preceding works on transport coefficient calculations in ac electric fields involving the Boltzmann equation, the time-dependent hydrodynamic regime is assumed to be described by a linear functional (a density gradient expansion) of the *instantaneous* number density. Justification for this assumption is given in the Appendix. In Sec. II we substantiate the existence of a time-dependent hydrodynamic regime, and identify the differences in the bulk and flux transport coefficients. The spherical harmonics decomposition of the Boltzmann equation of Robson and Ness [21] and subsequent Sonine polynomial expansion [22] (hereafter referred to as I) is then generalized to include an explicit time-dependence. In Sec. III we highlight the explicit effect of the nonconservative processes of attachment and ionization on the transport coefficients in ac electric fields over a large range of applied frequencies.

II. THEORY

The governing equation describing a swarm of charged particles moving through a background of neutral molecules in a time-dependent electric field is given by Boltzmann's equation for the phase-space distribution function $f(\boldsymbol{r},\boldsymbol{c},t)$:

$$\frac{\partial f}{\partial t}+\boldsymbol{c}\cdot\boldsymbol{\nabla} f+\frac{e\boldsymbol{E}(t)}{m}\cdot\frac{\partial f}{\partial \boldsymbol{c}}=-J(f). \tag{1}$$

Here $\boldsymbol{r}$ and $\boldsymbol{c}$ denote the position and velocity of the swarm particle at time t, respectively; e and m are the charge and mass of the swarm particle, respectively; and E is the electric field strength. We assume that swarm conditions prevail where the charged particle number density is much less than number density of the neutral species, rendering the collision operator linear in $f(\boldsymbol{r},\boldsymbol{c},t)$. The right hand side of Eq. (1) thus denotes the linear charged-particle-neutral-molecule collision operator, accounting for elastic, inelastic, superelastic, and nonconservative (e.g., ionizing, attaching, etc.) collisions. The details of the collision operators used are left to Sec. II D 3.

A. Time-dependent hydrodynamic regime

Experimental investigations of swarm behavior are generally made by sampling charged particle currents or charged particle densities:

$$n(\boldsymbol{r},t)=\int f(\boldsymbol{r},\boldsymbol{c},t)d\boldsymbol{c}. \tag{2}$$

The connection between experiment and theory is made through the equation of continuity

$$\frac{\partial n(\boldsymbol{r},t)}{\partial t}+\boldsymbol{\nabla}\cdot\boldsymbol{\Gamma}(\boldsymbol{r},t)=S(\boldsymbol{r},t), \tag{3}$$

where $\boldsymbol{\Gamma}(\boldsymbol{r},t)=n\langle\boldsymbol{c}\rangle$ is the swarm particle flux, and $S(\mathbf{r},t)$ represents the production rate per unit volume per unit time arising from nonconservative collisional processes.

In the context of static fields [23,24], transport coefficients are generally defined in connection with the hydrodynamic regime. This regime exists when the system has evolved to a stage independent of the initial state of the system *and* the space-time dependence of $f(\boldsymbol{r},\boldsymbol{c},t)$ and its velocity moments are expressible entirely in terms of linear functionals of $n(\boldsymbol{r},t)$. In consideration of transient effects and time-dependent fields there is an additional *explicit* source of time dependence in addition to the *implicit* time-dependence associated with the number density. To determine transport coefficients under these circumstances we assume a time-dependent hydrodynamic regime: The time-dependent hydrodynamic regime requires that the system has evolved to a stage where the spatial dependence of $f(\boldsymbol{r},\boldsymbol{c},t)$ and its moments are linear functionals of $n(\boldsymbol{r},t)$. A sufficient functional relationship between $f(\boldsymbol{r},\boldsymbol{c},t)$ (and associated velocity moments) and $n(\boldsymbol{r},t)$ in the time-dependent hydrodynamic regime is a density gradient expansion with time-dependent expansion coefficients

$$f(\boldsymbol{r},\boldsymbol{c},t)=\sum_{k=0}^{\infty} f^{(k)}(\boldsymbol{c},t)\odot(-\nabla)^k n(\boldsymbol{r},t), \tag{4}$$

where $f^{(k)}(\boldsymbol{c},t)$ are time-dependent tensors of rank k, and $\odot$ denotes a k-fold scalar product.

Assuming the functional relationship (4), the flux $\boldsymbol{\Gamma}(\boldsymbol{r},t)$ and source term $\boldsymbol{S}(\boldsymbol{r},t)$ in Eq. (3) are expanded as follows:

$$\boldsymbol{\Gamma}(\boldsymbol{r},t)=\boldsymbol{W}^{(\star)}(t)n(\boldsymbol{r},t)-\boldsymbol{D}^{(\star)}(t)\cdot\boldsymbol{\nabla} n(\boldsymbol{r},t), \tag{5}$$

$$S(\boldsymbol{r},t)=S^{(0)}(t)n(\boldsymbol{r},t)-\boldsymbol{S}^{(1)}(t)\cdot\boldsymbol{\nabla} n(\boldsymbol{r},t)+\boldsymbol{S}^{(2)}(t):\boldsymbol{\nabla}\boldsymbol{\nabla} n(\boldsymbol{r},t), \tag{6}$$

where $\boldsymbol{W}^{(\star)}(t)$ and $\mathbf{D}^{(\star)}(t)$ define the *flux* drift velocity and *flux* diffusion tensor, respectively. Substitution of expansions (5) and (6) into the continuity equation (3) yields the time-dependent *diffusion equation*,

$$\frac{\partial n}{\partial t}+\boldsymbol{W}(t)\cdot\boldsymbol{\nabla} n-\boldsymbol{D}(t):\boldsymbol{\nabla}\boldsymbol{\nabla} n=-R_a(t)n, \tag{7}$$

where we define the *bulk* transport coefficients

$$R_a(t)=-S^{(0)}(t) \quad \text{loss rate}, \tag{8}$$

$$\boldsymbol{W}(t)=\boldsymbol{W}^{(\star)}(t)-\boldsymbol{S}^{(1)}(t) \quad \text{bulk drift velocity}, \tag{9}$$

$$\mathbf{D}(t)=\mathbf{D}^{(\star)}(t)-\mathbf{S}^{(2)}(t) \quad \text{bulk diffusion tensor}. \tag{10}$$

We re-emphasize here that one should be cautious in the implementation of swarm data into fluid models when nonconservative collisional processes are involved. One should be aware of the differences in the definitions of both sets of transport coefficients, and ensure that the data employed in their theories is consistent with data required by their theory. The results in Sec. III demonstrate the often large differences in the magnitudes and profiles between the two sets of transport coefficients. Of course, in the absence of nonconservative processes, the bulk and flux transport coefficients coincide.

Expansion (4) was employed in the determination of ac swarm transport coefficients [10,14,16–18] without due con-

sideration (if at all) to the origin, approximations and limitations of such an expansion. In particular we highlight three important points.

(i) Such an expansion assumes the spatial dependence of all quantities is carried entirely by the *instantaneous* number density and its instantaneous spatial derivatives. The space-time variation of quantities is not influenced by the number density at times previous to this. The restrictions associated with this ''instantaneous density approximation'' are discussed in the Appendix.

(ii) Expansion (4) is just one way of representing f in the hydrodynamic regime. It is emphasized that Eq. (4) is a sufficient, but *not* necessary, condition in that sense. Such a representation is nevertheless mandatory if transport coefficients are to be defined. Expansion (4) is thus useful formally, though for practical purposes the expansion converges rapidly only for small gradients, and it would not be appropriate, for example, in sheath regions. A common misconception is that the hydrodynamic regime presupposes small gradients. It is the assumption of the functional form (4) which restricts the applicability to small gradients, not the assumption of a time-dependent hydrodynamic description per se. Such an expansion (or equivalent representation) is required whenever time-dependent hydrodynamic transport coefficients are to be calculated, as in the present paper.

(iii) The functional form (4) can also be generated through a perturbation or successive approximation solution of the Boltzmann equation by treating only the spatial derivative term as a perturbation. One should compare this with the Chapman-Enskog solution of the Boltzmann equation [25], which treats the entire left hand side of the Boltzmann equation (1) as the small term and the hydrodynamic solution [26] which treats only the temporal and spatial variation terms as small.

These points aside, once we establish the same functional form for the *spatial* dependence of the phase-space distribution function in the time-dependent hydrodynamic regime as that associated with the steady state case, the details of the spherical harmonic–Burnett function decomposition of the Boltzmann equation under time-dependent hydrodynamic conditions closely follow those associated with the steady state decomposition [21,22]. In what follows we briefly review the decomposition of the Boltzmann equation, highlighting the differences between the time-dependent and steady state procedures where appropriate.

B. Spherical harmonic decomposition of Boltzmann equation

The directional dependence of the phase-space distribution function in velocity space is represented in terms of a spherical harmonic expansion

$$f(\boldsymbol{r},\boldsymbol{c},t)=\sum_{l=0}^{\infty}\sum_{m=-l}^{l} f_m^{(l)}(\boldsymbol{r},c,t)Y_m^{[l]}(\hat{\boldsymbol{c}}), \tag{11}$$

where $\hat{\boldsymbol{c}}$ represents the angles of $\boldsymbol{c}$. In the time-dependent hydrodynamic regime, for our coordinate system, the spatial dependence is represented by

$$f_m^{(l)}(\boldsymbol{r},c,t)=\sum_{s=0}^{2}\sum_{\lambda=0}^{s} f(lm|s\lambda;c,t)G_m^{(s\lambda)}n(\boldsymbol{r},t), \tag{12}$$

where $G_m^{(s\lambda)}$ is the irreducible gradient operator [21]. Finally, the speed dependence of the above coefficients is represented by an expansion about a Maxwellian at an arbitrary *time-dependent* temperature $T_b(t)$, in terms of Sonine polynomials,

$$f(lm|s\lambda;c,t)$$

$$=w(\alpha(t),c)\sum_{\nu'=0}^{\infty} F(\nu' lm|s\lambda;\alpha(t),t)R_{\nu' l}(\alpha(t)c), \tag{13}$$

where

$$R_{\nu l}(\alpha(t)c)=N_{\nu l}\left(\frac{\alpha(t)c}{\sqrt{2}}\right)^{l} S_{l+1/2}^{(\nu)}\left(\frac{\alpha^2(t)c^2}{2}\right), \tag{14}$$

$$w(\alpha(t),c)=\left(\frac{\alpha^2(t)}{2\pi}\right)^{3/2}\exp\left\{-\frac{\alpha^2(t)c^2}{2}\right\}, \tag{15}$$

$$\alpha^2(t)=\frac{m}{kT_b(t)}, \tag{16}$$

$$N_{\nu l}^2=\frac{2\pi^{3/2}\nu!}{\Gamma(\nu+l+3/2)}, \tag{17}$$

and $S_{l+1/2}^{(\nu)}(\alpha^2(t)c^2/2)$ are Sonine polynomials. The requirement for a time-dependent zeroth-order approximation and details as to the choice of the convergence parameter $T_b(t)$ are left to Sec. II D 1. The moments $F(\nu lm|s\lambda;\alpha(t),t)$ satisfy the parity, symmetry, reality, and normalization conditions [I.4] and [I.5].

Using the orthonormality conditions of the spherical harmonics and modified Sonine polynomials, the following generalization to the time-dependent regime of the hierarchy of kinetic equations [I.16], [I.18], and [I.20] follows:

$$\sum_{\nu'=0}^{\infty}\sum_{l'=0}^{\infty}[\partial_t\delta_{\nu\nu'}\delta_{ll'}+n_0J_{\nu\nu'}^{l}(\alpha(t))\delta_{ll'}-R_a(t)\delta_{\nu\nu'}\delta_{ll'}$$
$$+ia(t)\alpha(t)(l'm10|lm)\langle\nu l\|K^{[1]}\|\nu' l'\rangle$$
$$-n_0J_{0\nu'}^{0}(\alpha(t))F(\nu l0|00;\alpha(t),t)$$
$$\times(1-\delta_{s0}\delta_{\lambda 0})\delta_{l'0}\delta_{m0}]F(\nu' lm|s\lambda;\alpha(t),t)$$
$$=\overline{X}(\nu lm|s\lambda;\alpha(t),t), \tag{18}$$

$$(\nu,l)=0,1,2,\ldots,\infty,\quad |m|\leq\min\{l,\lambda\},\quad s+\lambda=\text{even},$$

where R_a is the attachment rate, and is discussed in Sec. II D 2. The right hand side vectors remain unchanged (aside from the time dependence in the moments), and explicit expressions for the required members are given by Eqs. [I.16], [I.18], and [I.20]. The reduced matrix elements of the collision operator, velocity derivative, and velocity are given by Eqs. [I.11], [I.12a], and [I.12b], respectively.

The only explicit difference in the hierarchies of kinetic equations associated with the static hydrodynamic and time-dependent hydrodynamic regimes is the inclusion of the partial time-derivative operator in the coefficient matrix. The ramification of this on the spatially homogeneous member

$(s,\lambda=0,0)$ of the hierarchy is particularly striking. In the presence of nonconservative processes *and* a time-varying field (no matter how slight), this member is no longer a true eigenvalue problem. The implications of the physical interpretation of the spectrum of eigenvalues in the steady state problem [21] do not appear to carry over. In the periodic steady state, Floquet theory [27] may give relations to these eigenvalues, but this is by no means obvious.

An implicit finite difference scheme is employed to evaluate the partial time derivatives in (18). It is advantageous to discretize in time at this final stage, to avoid the approximations associated with finite differencing the continuity equation. Discretizing in time at the nth time step, each element of the hierarchy is evaluated at the same basis temperature T_b^n. If the time step is Δt, then the partial derivative at the nth time step is approximated by

$$\left.\frac{\partial}{\partial t}F(\nu lm|s\lambda;\alpha(t),t)\right|_{\alpha=\alpha_n,t=n\Delta t} = \frac{F^n_{\alpha_n}(\nu lm|s\lambda)-F^{n-1}_{\alpha_n}(\nu lm|s\lambda)}{\Delta t}, \tag{19}$$

where

$$F^b_{\alpha_a}(\nu lm|s\lambda)=F(\nu lm|s\lambda;\alpha(t_a),t_b). \tag{20}$$

The quantity $F^{n-1}_{\alpha_n}(\nu lm|s\lambda)$ is expressed in terms of the calculated moment at the $(n-1)$th step $F^{n-1}_{\alpha_{n-1}}(\nu lm|s\lambda)$, via the linear relation [28]

$$F^{n-1}_{\alpha_n}(\nu lm|s\lambda)=\sum_{\nu'=0}^{\nu} A^l_{\nu\nu'}(\mu_{nn-1})F^{n-1}_{\alpha_{n-1}}(\nu' lm|s\lambda), \tag{21}$$

where

$$A^l_{\nu\nu'}(\mu_{ij})=\frac{\overline{N}_{\nu' l}}{\overline{N}_{\nu l}}\mu_{ij}^{\nu'+1/2l}\frac{(1-\mu_{ij})^{\nu-\nu'}}{(\nu-\nu')!} \tag{22}$$

$$\mu_{ij}=\left(\frac{\alpha_i}{\alpha_j}\right)^2, \quad N^2_{\nu l}=\frac{2\pi^{3/2}}{\nu!\Gamma(\nu+l+3/2)}=\frac{1}{(\nu!)^2}N^2_{\nu l}. \tag{23}$$

Consistency requires

$$A^l_{\nu\nu'}(1)=\delta_{\nu\nu'}. \tag{24}$$

C. Transport properties

The transport coefficients are related to the calculated moments via

$$R^n_a=n_0\sum_{\nu'=0}^{\infty} J^0_{0\nu'}(\alpha_n)F^n_{\alpha_n}(\nu'00|00), \tag{25}$$

$$W^n=\frac{i}{\alpha_n}F^n_{\alpha_n}(010|00)-in_0\sum_{\nu'=1}^{\infty} J^0_{0\nu'}(\alpha_n)F^n_{\alpha_n}(\nu'00|11), \tag{26}$$

$$D^n_L=-\frac{1}{\alpha_n}F^n_{\alpha_n}(010|11)-n_0\sum_{\nu'=1}^{\infty} J^0_{0\nu'}(\alpha_n)[F^n_{\alpha_n}(\nu'00|20) -\sqrt{2}F^n_{\alpha_n}(\nu'00|22)], \tag{27}$$

$$D^n_T=-\frac{1}{\alpha_n}F^n_{\alpha_n}(011|11)-n_0\sum_{\nu'=1}^{\infty} J^0_{0\nu'}(\alpha_n)\left[F^n_{\alpha_n}(\nu'00|20) +\frac{1}{\sqrt{2}}F^n_{\alpha_n}(\nu'00|22)\right], \tag{28}$$

where the components involving summations constitute the explicit nonconservative effects on the transport coefficients, while the remainder constitute the flux contribution.

The spatially homogeneous mean energy $\varepsilon(t)$ and the gradient energy vector $\gamma(t)$ [16,17], defined through a density gradient expansion of the average energy $\epsilon(\boldsymbol{r},t)$,

$$\epsilon(\boldsymbol{r},t)=\frac{1}{n(\boldsymbol{r},t)}\int\frac{1}{2}mc^2 f(\boldsymbol{r},\boldsymbol{c},t)d\boldsymbol{c}=\varepsilon(t)+\boldsymbol{\gamma}(t)\cdot\frac{\boldsymbol{\nabla}n}{n} +\ldots, \tag{29}$$

play pivotal roles in a qualitative understanding of the temporal profiles of the drift and diffusion coefficients. The gradient energy parameter $\boldsymbol{\gamma}$ describes the first order spatial variation of the average energy through the swarm. These quantities in a Burnett function basis are given by

$$\varepsilon^n=\frac{3}{2}kT_b^n\left[1-\sqrt{\frac{2}{3}}F^n_{\alpha_n}(100|00)\right], \tag{30}$$

$$\gamma^n=\frac{3}{2}kT_b^n\left[i\sqrt{\frac{2}{3}}F^n_{\alpha_n}(100|11)\right]. \tag{31}$$

As we can see, solution of the hierarchy to second order in the density gradients is sufficient to yield all quantities addressed in this section.

This ends the general theoretical decomposition of the Boltzmann equation in the time-dependent hydrodynamic regime. In Sec. II D we discuss the numerical aspects of the solution of hierarchy (18).

D. Numerical solution of the hierarchy

1. Truncation, convergence, and choice of T_b

Numerical solution of Eq. (18) requires truncation of the ν and l summations to manageably finite values $\nu_{\max}$ and $l_{\max}$, respectively. The values of $l_{\max}$ and $\nu_{\max}$ required to satisfy some convergence criteria represent the deviation of the velocity distribution from spherical symmetry and the deviation of the speed distribution from a Maxwellian distribution at T_b (in some sense), respectively. In general, a single T_b is sufficient only to ensure convergence over a limited range of E/n_0 or equivalently ε. Hence in time-dependent situations where the field (or mean energy) falls outside these limits, the use of a single basis temperature will in general fail. For quite general applications, the weighting function must subsequently be allowed to vary in time to accommodate this. The scheme for computing the basis temperature at each step

must be fully automated and self-consistent, and minimize the number of basis temperatures used (since the evaluation of the collision matrix for each T_b is computationally expensive). At a given time step, we assume an initial estimate of the basis temperature to be that from the previous time step. The convergence in the ν index is then considered over a range of $\nu_{\max}$ values. Failure to meet the convergence criteria results in a new T_b, and the convergence checks are repeated. We alternately iterate T_b either side away from the initial estimate of T_b until the convergence criteria is satisfied. This technique ensures a predefined accuracy of the transport coefficients and/or distribution function coefficients in the ν index for a defined $l_{\max}$ value. The value of $l_{\max}$ is then incremented until some convergence criteria is satisfied over the whole temporal profile.

2. Form and solution of the hierarchy

Solution for the transport coefficients under consideration (up to diffusion in the presence of nonconservative processes) requires the solution of five members of the hierarchy determined by $(s,\lambda,m)=(0,0,0)$, $(1,1,0)$, $(1,1,1)$, $(2,0,0)$, and $(2,2,0)$. The order of solution of members (defined by the m index) within a given level of the hierarchy [defined by (s,λ)] is arbitrary.

In contrast to the steady state, the spatially homogeneous member of the hierarchy $(s,\lambda,m)=(0,0,0)$ represents a system of coupled nonlinear equations, and is solved iteratively for the moments $F^n_{\alpha_n}(\nu lm|00)$ and the loss rate R_a. This technique was found to be robust, and forms a first test on the suitability of the chosen T_b. The remaining members of the hieararchy can be solved via direct numerical inversion. The coefficient matrix exhibits a tridiagonal block structure, with off-diagonal blocks sparse. We employ a sparse matrix routine to exploit this property.

3. Collision operators and calculation of the collision matrix

For elastic interactions we use the original Boltzmann collision operator [29], while for inelastic and superelastic collision we prefer the semiclassical generalization of Wang-Chang *et al.* [30]. The attachment and ionization collision operators employed are detailed in Ref. [21]. No restriction is made concerning the anisotropy of the scattering cross-sections.

The calculation of the collision matrix for the ''two-temperature'' moment theory has been developed extensively over the last 20 years, and is quite general in its applicability. In particular we use the elegant Talmi transformation methods of Kumar [31], which allow the separation of mass and interaction effects. This is particularly important in that we are not restricted to small mass ratios m/m_0, and as such the code is applicable to ions as well (subject to the applicability of the two-temperature theory). A discussion of the calculation of the collision matrix is beyond the scope of this paper, and the reader is referred to Refs. [31,32].

III. RESULTS

In this section we investigate the transport properties of an isolated swarm undergoing model attachment and ionization interactions with a series of gases under the influence of an ac electric field. The motivation for employing model swarm-particle-neutral molecule interactions lies in the fact that they can provide an unambiguous test of the validity and accuracy of various theories, since cross sections are specified analytically. In addition, by virtue of the simple form of the cross sections in these models, they provide a means to isolate and elucidate physical phenomena and processes which occur in real systems but which may be obscured by other interaction processes present. It must be emphasized, however, that the theory and associated computer code are equally valid for *real* cross sections. The emphasis of this section is the observation and physical interpretation of the properties of the instantaneous and cycle-averaged values of transport coefficients. In doing so, we hope to provide benchmarks for future investigations of charged particle swarms in ac electric fields.

The quantities calculated in the following sections are functions of reduced angular frequency (ω/n_0, where ω is the angular frequency of the electric field and n_0 is the neutral number density). Typical plasma processing conditions (e.g., pressure of 0.1 Torr and a frequency of 13.56 MHz, with a neutral gas temperature $T_0=293$ K) correspond to a value of the reduced angular frequency of 2.6×10^{-14} rad m^3 s^{-1}).

A. Power law attachment model

The power law attachment model is defined by [22]

$$\sigma_{el}(\epsilon)=10\epsilon^{-1/2}\ \text{Å}^2 \quad \text{(elastic cross section)},$$

$$\sigma_A(\epsilon)=a\epsilon^p\ \text{Å}^2 \quad \text{(attachment cross section)},$$

$$E/n_0=0.4\cos\omega t\,\text{Td} \quad \text{where 1 Td}=10^{-21}\ \text{V m}^{-2}, \tag{32}$$

$$m_0=16\,\text{amu},$$

$$T_0=293\,\text{K},$$

where ϵ is in units of eV. All scattering is assumed isotropic. The validity of the time-dependent code was established by applying it to the steady state dc electric field problem. Accuracies to within 0.1% were found for all coefficients over all values of the a and p considered.

In Figs. 1–7 we display the variation of the periodic steady state profiles of the transport properties for electrons in the model attaching gas for various attachment amplitudes and field frequencies. We display only the power laws $p=0.5$ and -1. The benchmark for this gas is the case where $p=-1/2$. Here the attachment collision frequency is independent of energy and all transport coefficients and transport properties [aside from the attachment rate $R_a(t)$] were found to be independent of the attachment amplitude. In addition the bulk transport coefficients were found to be equal to the flux coefficients [i.e., $W(t)=W^{(*)}(t)$, $n_0D_L(t)=n_0D_L^{(*)}\times(t)$, and $n_0D_T(t)=n_0D_T^{(*)}(t)$]. This result and the origins of it are well known for the dc steady state case, and carry over directly to the ac case. These results support the numerical integrity of the present code in the presence of attachment processes.

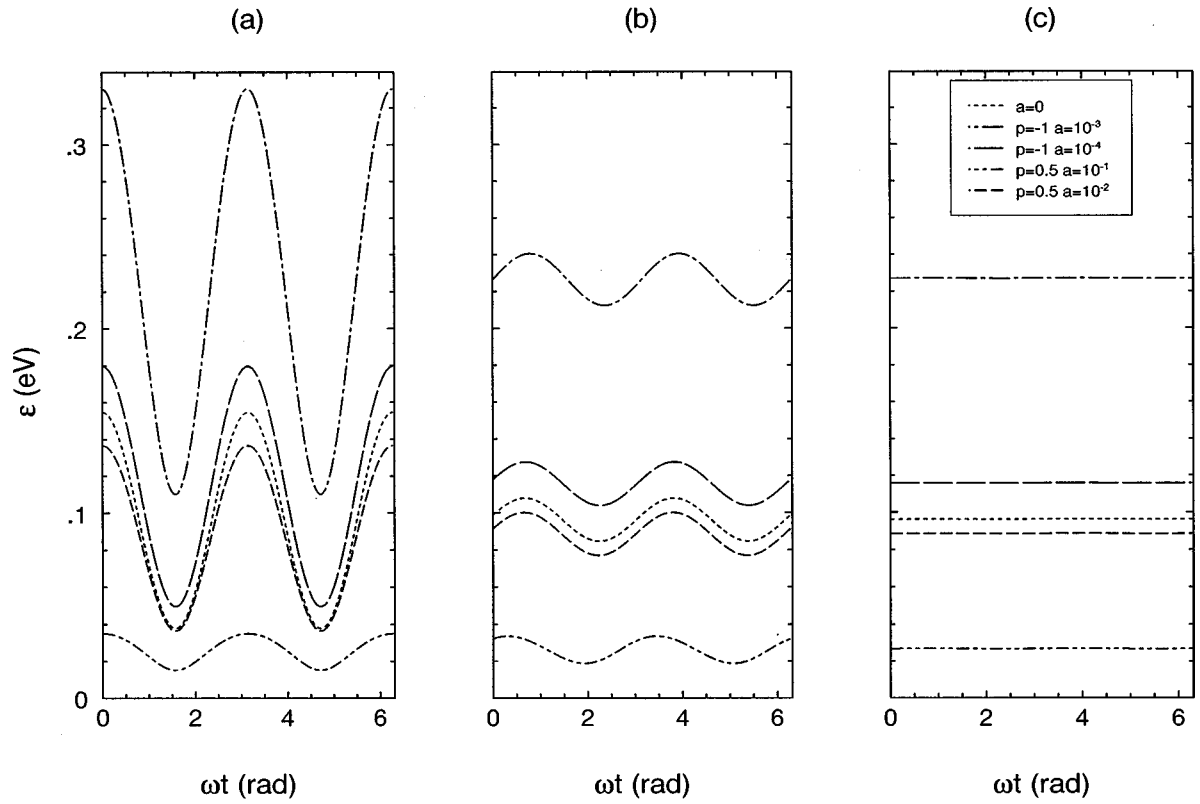

FIG. 1. Temporal variation of the spatially homogeneous mean energy for the power law attachment model (32) for various attachment amplitudes and power laws as a function of applied frequency ω/n_0 (rad m^3 s^{-1}): (a) 1×10^{-21}, (b) 1×10^{-17}, and (c) 1×10^{-15}.

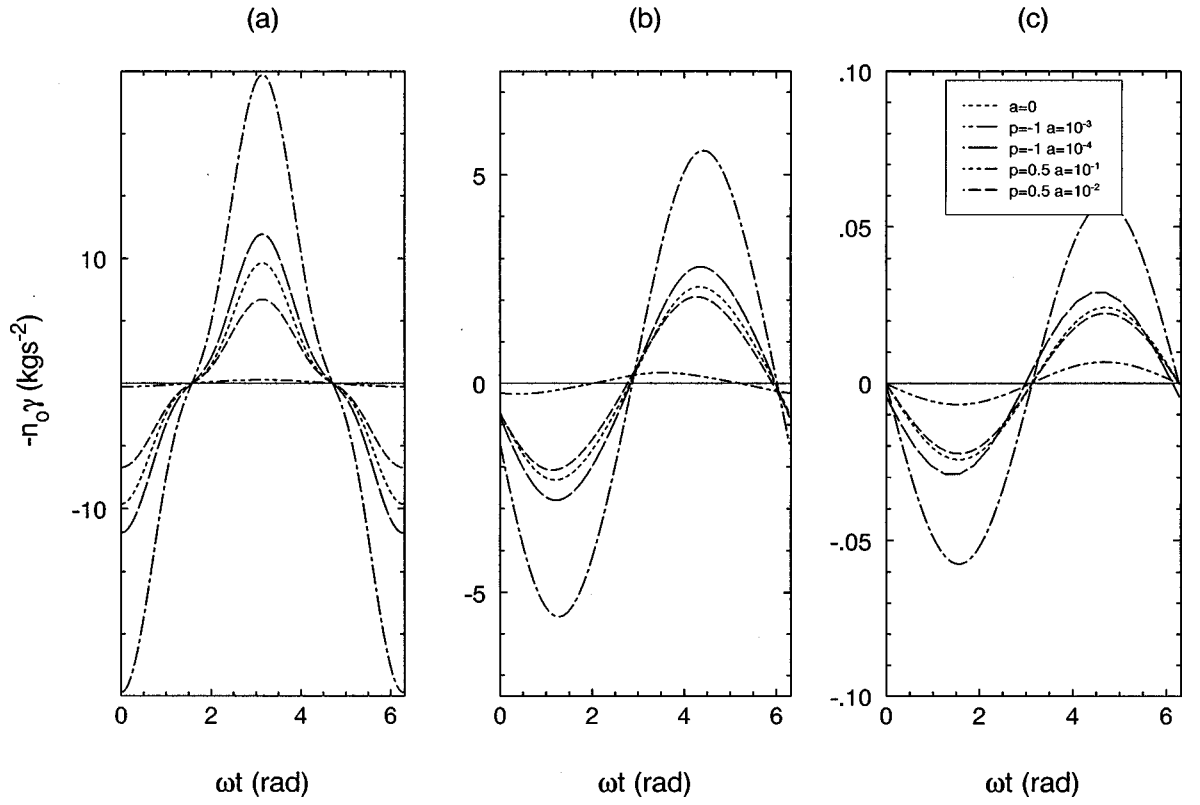

FIG. 2. Temporal variation of the gradient energy parameter for the power law attachment model (32) for various attachment amplitudes and power laws as a function of applied frequency ω/n_0 (rad m^3 s^{-1}): (a) 1×10^{-21}, (b) 1×10^{-17}, and (c) 1×10^{-15}.

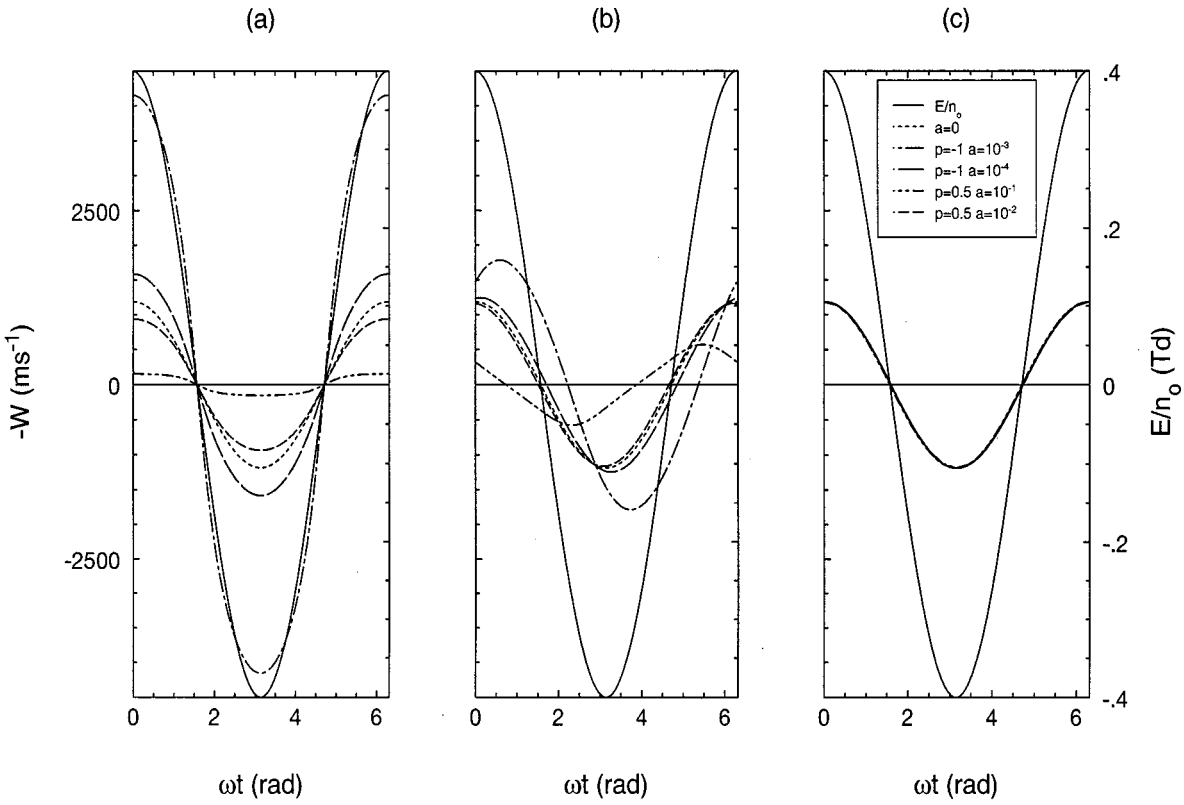

FIG. 3. Temporal variation of the $a=0$ drift velocity and bulk drift velocity for the power law attachment model (32) for various attachment amplitudes and power laws as a function of applied frequency ω/n_0 (rad m^3 s^{-1}): (a) 1×10^{-21}, (b) 1×10^{-17}, and (c) 1×10^{-15}.

Figure 1 shows the temporal variation of the mean energy ε, with attachment amplitude and power law for three applied reduced angular frequencies ω/n_0. The conservative case is represented by the $a=0$ profile. Consider the low-frequency case [Fig. 1(a)]. For $p=0.5$, the attachment collision frequency increases with energy. This preferential attachment of the higher energy electrons gives rise to the phenomenon of attachment cooling (i.e., the reduction in the mean (or swarm averaged) energy due to attachment) [22]. The cooling action is strengthened with increasing attachment amplitude. In contrast, for $p=-1$, the attachment collision frequency decreases with energy and the predominant removal of the lower energy electrons result in an increase in the mean energy, i.e., attachment heating. The variation of these profiles with frequency, i.e., the reduction in the amplitude of the modulation and the increase in the phase lag with respect to the field, follows directly from well known arguments (see, e.g., Refs. [6, 8–12, 15–18, 33]). They essentially result from the inability of the swarm averaged properties to respond (here with a time scale of ν_e^{-1} where ν_e is the energy transfer collision frequency) to changes in the field (a time scale of ω^{-1}). However, we note the small variations in the amplitude of oscillations and phase lag with power law and attachment amplitude, which correspond to

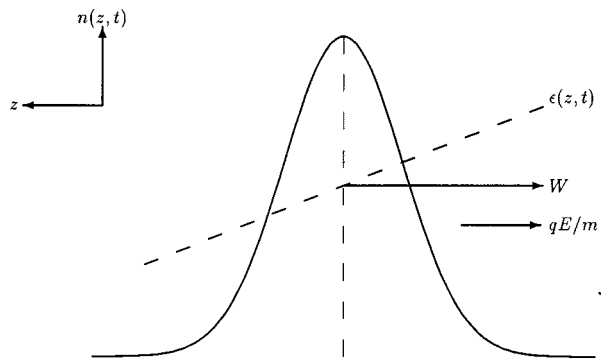

FIG. 4. Schematic representation of a pulse of charged particles drifting in a dc electric field with center-of-mass velocity W. The mean energy $\epsilon(z,t)$ is also shown in a schematic way.

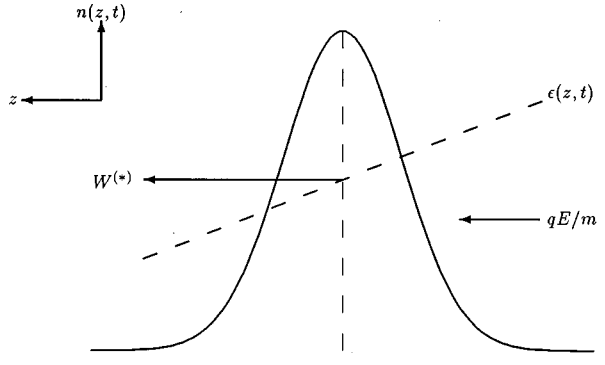

FIG. 5. Schematic representation of a pulse of charged particles in response to a change in the field direction where $W^{(*)}$ and all local instantaneous drift velocities along the pulse have changed sign before γ.

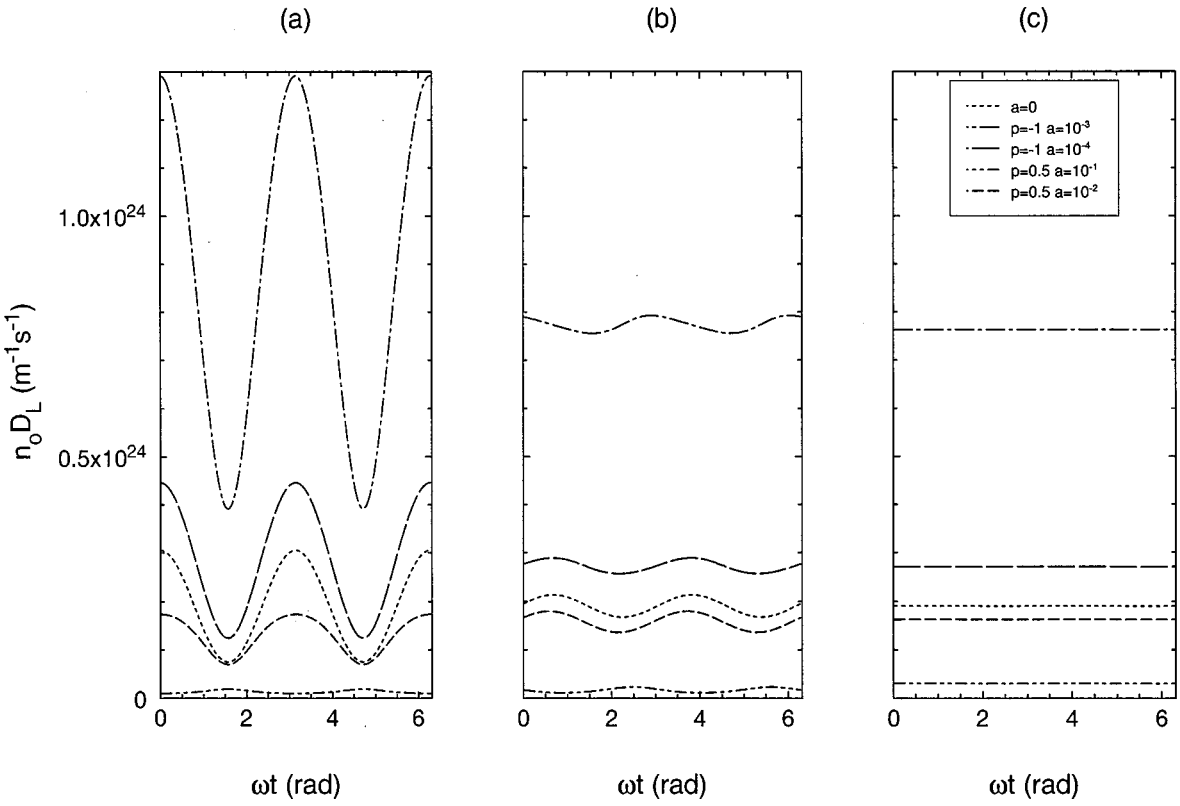

FIG. 6. Temporal variation of the attachment free and bulk longitudinal diffusion coefficients for the power law attachment model (32) for various attachment amplitudes and power laws as a function of applied frequency ω/n_0 (rad m^3 s^{-1}): (a) 1×10^{-21}, (b) 1×10^{-17}, and (c) 1×10^{-15}.

the variation in the total energy transfer collision frequency with a and p.

The temporal variation of the gradient energy parameter γ has important implications for the temporal profiles of the bulk drift velocity considered later. In the steady state dc case, it is well known that the average energy of the swarm increases through the swarm in the direction of the drift [16–18,34,35], since electrons at the front of the swarm have generally fallen through a greater potential. This carries directly over to the quasi-dc or low-frequency regime [viz. the $a=0$ profile in Fig. 2(a)]. In this frequency regime, for attachment cooling $p=0.5$, as expected the preferential removal of high energy electrons from the front of the swarm results in a suppression of the spatial variation in the energy through the swarm while the converse applies for attachment heating. Independent of the power law considered, an increase in the frequency of the applied field results in a decrease in the amplitude of modulation and an increase in the phase lag with respect to the field, indicating an inability of this parameter to relax fully before the field changes. More specifically we note that the relaxation time associated with this parameter is decreased with increasing a for attachment cooling, while the converse applies for attachment heating. These results are indicated by the appropriate phase lags. It is important to note that, in the high frequency limit [viz. Fig. 2(c)], independent of the power law, the amplitude of the spatial variation of the average energy through the swarm decreases rapidly to zero. Essentially, in the high frequency regime, there is insufficient time for any spatial variation to be generated before the field changes, and thus (to first order in spatial gradients) the average energy is constant throughout the swarm.

The temporal profiles of the bulk drift velocity are displayed in Fig. 3. For both power law models, over the range of attachment amplitudes considered here, there is little variation in $W^{(*)}$ with a, indicating the implicit effect of attachment on the drift velocity is weak for this model. The flux drift velocity is thus approximately equal to the drift velocity when conservative processes only are present. For clarity we present only the conservative property in Fig. 3 and not the various flux drift profiles.

In the low frequency regime [viz. Fig. 3(a)], for attachment cooling ($p=0.5$) the instantaneous bulk drift velocity has a lower magnitude as compared with the flux drift velocity, and the amplitude of bulk drift velocity decreases with increasing attachment amplitude. The converse applies for attachment heating. The origin of this behavior is well known in dc steady state systems, and carries directly over to the quasi-dc regime [22,35,36]. There exist two components which contribute to the bulk drift velocity (or equivalently velocity of the center of mass (CM) of the swarm): (1) the net transport of the CM of the swarm brought about solely by the electric field force ($W^{(*)}$); and (2) the net transport of the CM of the swarm brought about by energy selective nonuniform creation or annihilation [$\boldsymbol{S}^{(1)}(t)$]. Figure 2(a) shows that the spatial variation of the average energy increases through the swarm in the direction of the drift velocity and this is portrayed schematically in Fig. 4. For attachment cooling $p=0.5$, preferential attachment of the higher energy

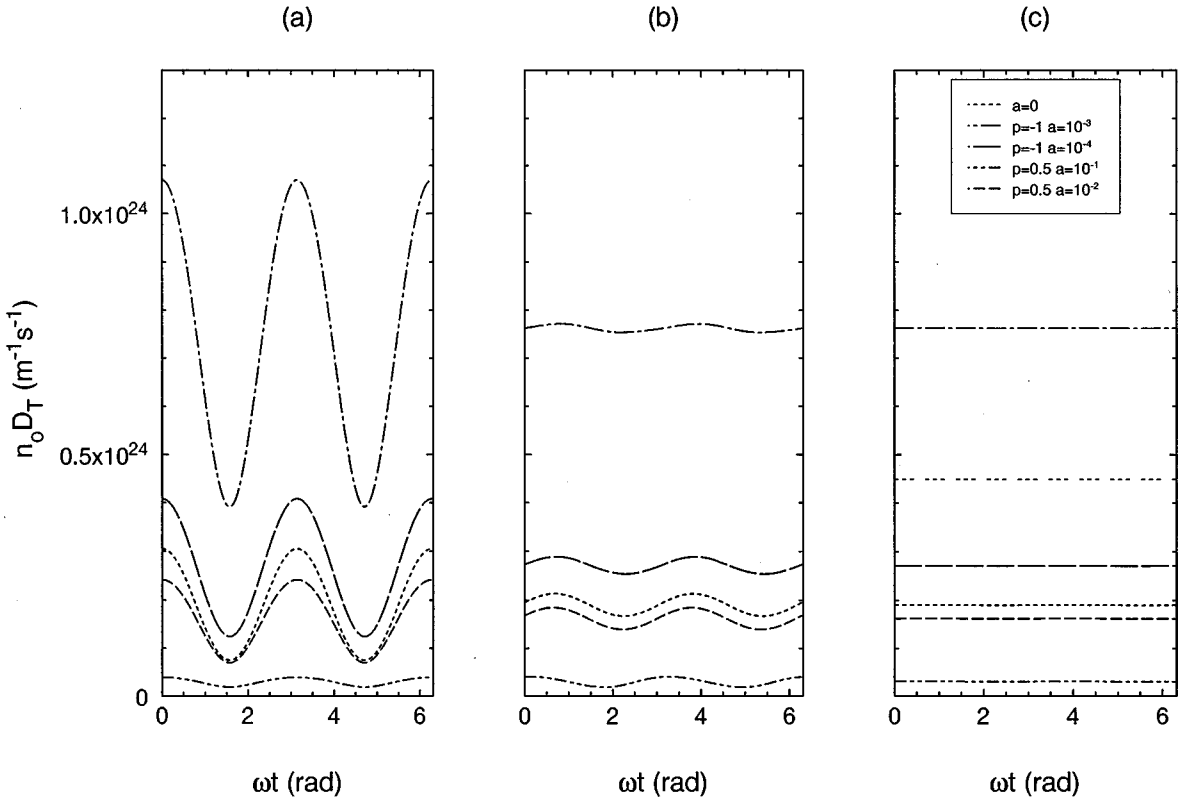

FIG. 7. Temporal variation of the attachment free and bulk transverse diffusion coefficients for the power law attachment model (32) for various attachment amplitudes and power laws as a function of applied frequency ω/n_0 (rad m^3 s^{-1}): (a) 1×10^{-21}, (b) 1×10^{-17}, and (c) 1×10^{-15}.

electrons from the front of the swarm will result in a shifting of the center of mass of the swarm in a direction opposite to the flux drift velocity (or equivalently the electric field force). The decrease in the magnitude of the bulk (CM) velocity of the swarm as compared with the flux drift velocity at all phases of the field then follows. Conversely, for $p=-1.0$, preferential attachment of the lower energy electrons from the tail of the swarm acts to shift the center of mass in the direction of the flux drift (electric field force), and subsequently the magnitude of the bulk drift velocity at all phases of the field is increased as compared with the flux drift velocity profile. At this frequency, at phases where $E=0$, $\gamma=0$, and hence $W=W^{(*)}$.

When the frequency of the applied field is increased however [viz. Fig. 3(b)], anomalous properties arise. For attachment cooling ($p=0.5$), the bulk drift velocity has a ''negative'' phase lag with respect to the applied field, i.e., the bulk drift velocity appears to preempt changes in the field. This negative phase lag increases for increasing attachment amplitudes. In contrast for attachment heating ($p=-1.0$), we have a positive phase lag in spite of the applied frequency satisfying the criterion $\omega/n_0 \ll \nu_m/n_0$ over the entire cycle of the field. The traditional explanations for describing the variation of the drift velocity with frequency appear to fail under these circumstances. This phenomenon arises from the inability of the spatial variation of the average energy to relax sufficiently quickly to follow changes in the field as shown in Fig. 2(b). Let us consider only attachment cooling initially ($p=0.5$). As the field decreases in magnitude, a situation is reached where the inability of $\gamma(t)$ to relax results in the magnitude of net motion of the center of mass brought about only by preferential attachment of low energy electrons being greater in magnitude and opposite in direction (as discussed previously) to the net drift brought about by the field. The center-of-mass drift velocity thus changes direction before the field changes and the negative phase lag in the bulk drift velocity for this model follows. Essentially (for $\nu_m \gg \omega$), the flux drift velocity is in phase with the field, while the nonconservative component of the bulk drift velocity is in phase with $\gamma(t)$. In the phase of the field where $W^{(*)}(t)\gamma(t)>0$ (portrayed schematically in Fig. 5), we have the anomalous situation where the flux drift velocity $W^{(*)}(t)$ and the net transport brought out by preferential attachment of high energy electrons are in the same direction. As a result in this phase, $|W^{(*)}(t)|<|W(t)|$, in contrast to steady state dc results. The instantaneous bulk and flux drift velocity are equal at phases of the field where $\gamma(t)=0$. Here no preferential spatial annihilation exists, and subsequently no motion of the center of mass of the electrons can result. Similar arguments can be used to explain the ''enhanced positive'' phase lag in the drift velocity for attachment heating.

In the high frequency regime it is evident from Fig. 3(c) that instantaneously the *bulk* drift velocity approaches the *flux* drift velocity, for both attachment power laws and all attachment amplitudes considered here. We predict this phenomenon is independent of nonconservative processes at high frequencies. Physically, at these frequencies there is insufficient time for any spatial variation in the average energy to be established at any phase of the cycle [viz. Fig. 2(c)].

Subsequently, there is no preferential spatial attachment from any region of the swarm, and it follows that there is no net motion of the center of mass brought about by nonconservative processes.

To conclude our discussion of attachment processes in ac electric fields, we comment on the temporal profiles of the bulk and flux longitudinal and transverse diffusion coefficients shown in Figs. 6 and 7, respectively. The variation of the flux diffusion coefficients with attachment amplitude, power law and frequency (i.e., the implicit effect of attachment on diffusion) reflect those associated with the mean energy. Until recently [37], very little was known concerning the physical origins of the variation of the bulk diffusion coefficients with nonconservative processes, even for the steady state dc case. These variations are associated with not only first order spatial variation of the average energy (γ), but also second order symmetric variations and involve the coefficients associated with a second order expansion of the average energy [Eq. (29)]. At this stage we do not attempt to explain the phenomenon associated with the bulk diffusion coefficients, but merely highlight some interesting phenomena associated with them. We note both $n_0 D_L$ and $n_0 D_T$ show an enhancement or reduction in the cycle-averaged value with attachment amplitude for attachment heating or cooling at low frequencies. The modulation of all profiles decreases to zero in the high frequency limit. Importantly, our results indicate the inadequacies of assuming an isotropic diffusion tensor; there are appreciable differences in amplitude and phase of the profiles for diffusion parallel and perpendicular to the electric field. The temporal profile of $n_0 D_T$ has a greater phase lag with respect to the field as compared with $n_0 D_L$. At low frequencies [viz. Fig. 6(a)], it is also interesting to note the antiphase behavior in $n_0 D_L(t)$ for attachment cooling and $a = 1 \times 10^{-1}$ Å^2 (eV)$^{-1/2}$, as compared with lower attachment amplitudes for $p = 0.5$ and all attachment amplitudes of $p = -1.0$. Importantly, the instantaneous *bulk* diffusion coefficients approach the instantaneous *flux* diffusion coefficients as frequency is increased.

B. Ionization model of Lucas and Saelee

For the consideration of ionization processes we employ the benchmark model of Lucas and Saelee [38]:

$$\sigma_{el}(\epsilon) = 4\epsilon^{-1/2} \text{ Å}^2 \quad \text{(elastic cross section)},$$

$$\sigma_{ex}(\epsilon) = \begin{cases} 0.1(1-F)(\epsilon - 15.6) \text{ Å}^2, & \epsilon \geqslant 15.6 \text{ eV} \quad \text{(inelastic cross section)} \\ 0, & \epsilon < 15.6 \text{ eV}, \end{cases}$$

$$\sigma_I(\epsilon) = \begin{cases} 0.1F(\epsilon - 15.6) \text{ Å}^2, & \epsilon \geqslant 15.6 \text{ eV} \quad \text{(inonization cross section)} \\ 0, & \epsilon < 15.6 \text{ eV}, \end{cases}$$

$$P(q, \epsilon') = 1, \tag{33}$$

$$m/m_0 = 10^{-3},$$

$$E/n_0 = 10 \cos \omega t \text{ Td},$$

$$T_0 = 0 \text{ K}.$$

Here ϵ is defined in units of eV. Elastic and inelastic scattering is assumed to be isotropic. For ionization our collision operator assumes a zeroth order trunction in the mass ratio m/m_0. The ionization partition function $P(q, \epsilon')$ then describes the partitioning of the available energy between the scattered and ejected electrons. When set to unity indicates that all fractions of the distribution of the energy available after the ionization process are equally probable. For the low ionization rates consider here, the transport coefficients are relatively insensitive to the values of this partitioning function. For high ionization rates, an accurate knowledge of the partitioning of the available energy between the incident and ejected electrons is required [22]. This model has been extensively investigated in dc steady state systems [22,36,38,39].

It is common in the literature on ac swarms to find ionization processes simply treated as a another inelastic process (see, e.g., Refs. [8,11] and others). Subsequently, discussions on the effect of ionization on relaxation are generally framed in terms of a single ionization collision frequency. Mathematically this quantity represents only the inelastic effect of an ionization process and does not consider the explicit effect of the ejected electron. The interesting aspect of this model is that the total cross section (elastic, inelastic, and ionization) is constant independent of the parameter F. This model thus represents a good test on the validity of such an assumption.

The variation of the mean energy and the ionization rate with frequency for three values of the parameter F are displayed in Figs. 8(a) and 8(b), respectively. The phenomenon of ionization cooling of the swarm is well known [22,36] in dc electric fields, and is shown in Fig. 8(a) to carry over directly to the ac case. This phenomenon is independent of the functional form of the ionization cross section, but is strengthened with increasing ionization rate. Essentially, the available post-collision energy is now distributed over an

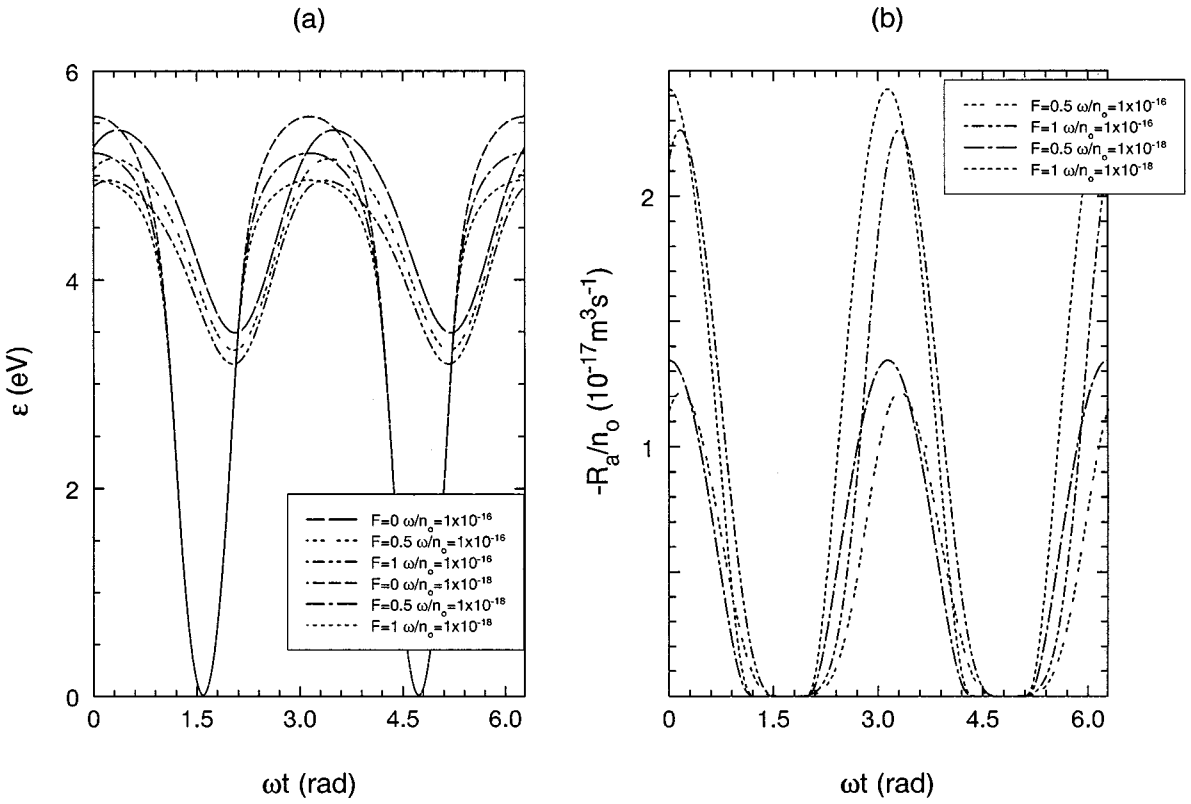

FIG. 8. Temporal variation of (a) spatially homogeneous mean energy, and (b) ionization rate for the Lucas-Saelee ionization model (33) for various values of F and applied frequencies ω/n_0 (rad m^3 s^{-1}).

increased number of electrons, and the average energy of the swarm must therefore decrease. At higher frequencies the amplitude of modulation and the phase lags for varying F values are considerably different, yet the total cross section remains constant. These indicate that ionization has a significant influence on the relaxation properties of the swarm even for the low ionization rates considered here. We should emphasize that the variation of the phase lag with F is not just an implicit effect on the relaxation time due to the cooling action of ionization. The phase lag *reduces* with increasing ionization, in contrast to the increase in the relaxation time (decrease in the inelastic collision frequency) which would be associated with the cooling effect.

As for the attachment case considered in Sec. III A, the temporal variation of the gradient energy parameter is pivotal to discussions of the bulk and flux drift velocities. This parameter is displayed in Figs. 9(a) and 9(b). The profile in Fig. 9(a) shows the signature effect of threshold inelastic processes with the significant reduction in the magnitude of $\gamma(t)$. We also observe that increasing F acts to further reduce the spatial variation in the average energy through the swarm. In addition to the inelastic nature of ionization scatterings, the residual incident energy is also essentially shared between the scattered and ejected electrons. Both processes act to reduce the average energy in that region of configuration space where the ionization process has occurred. For this model, ionization occurs predominantly at the leading edge of the swarm and the reduction in the spatial variation in the average energy through the swarm due to ionization follows. Using similar arguments, it follows at higher frequencies, the phase lag of $\gamma(t)$ is reduced with increasing F, as shown in Fig. 9(b).

Figures 10(a) and 10(b) display the flux and bulk drift velocity at two different applied frequencies for three values of F. For this model, the implicit effect of ionization on the drift velocity is weak, and the flux components for both F values are essentially equal to the $F=0$ profiles. As expected in the phases of the field where the ionization rates are low, the bulk and flux drift velocities are equal. We observe an increase in the instantaneous values of the bulk drift as compared with the flux drift when F, and hence the ionization collision frequency is increased. Here, since the ionization collision frequency increases with energy, in general more electrons are created at the front of the swarm and thus the ionization processes act to shift the center of mass of the swarm in the direction of the flux drift. At higher frequencies we note a phase shift in the region where the flux and bulk drift differ due to the phase shift in the ionization rate with respect to the electric field as shown in Fig. 8(b). We also note an increase in the amplitude of the bulk drift velocity profiles with frequency. This increase is a result of the increase (between the two applied frequencies) in the instantaneous values of $\gamma(t)$ in the phases of the field where significant ionization processes occur. We expect that only when the frequency of the applied field is such that there is significant ionization processes acting when the field changes directions will there be a positive phase lag in the bulk drift velocity, for reasons similar to those discussed in Sec. III A.

The flux and bulk longitudinal diffusion coefficients are displayed for this model in Figs. 11(a) and 11(b) for two frequencies. As for the attachment model, the flux diffusion coefficients essentially follow the same variation with frequency and F as that shown by the mean energy. For this model, bulk longitudinal (as well as transverse) diffusion is

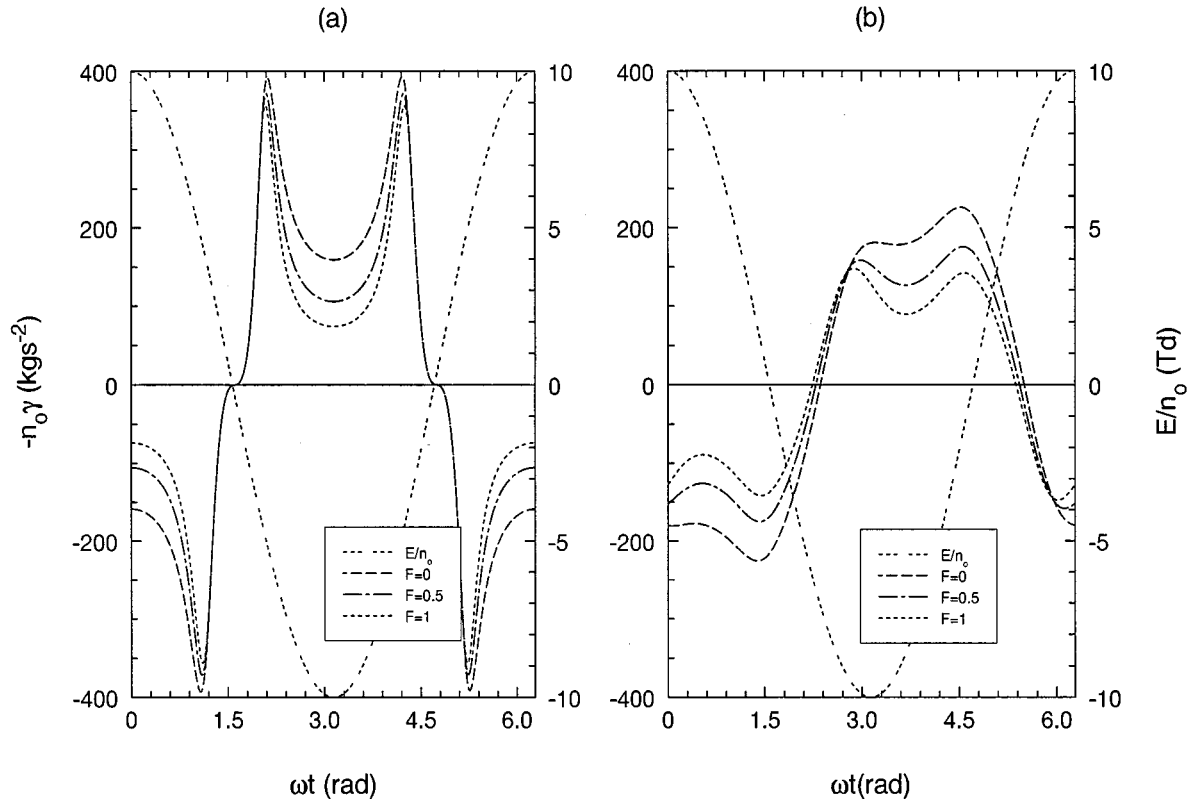

FIG. 9. Temporal variation of the gradient energy parameter for the Lucas-Saelee ionization model (33) for various values of F and applied frequencies ω/n_0 (rad m^3 s^{-1}): (a) 1×10^{-18}; (b) 1×10^{-16}.

enhanced in the regions where significant ionization occurs. For higher frequencies, the appearance of a spike in the bulk longitudinal diffusion profiles is indicative of an inability of the transport property to relax in combination with a nonmonotonically relaxing transport property. To understand this variation fully, one must return to and understand the relaxation characteristics associated with this coefficient (see Ref. [33] for a detailed discussion).

IV. CONCLUDING REMARKS

In this work we have presented a systematic investigation of the influence of nonconservative collisional processes on transport coefficients of charged particles in gases under the influence of an ac electric field at various applied frequencies. We have (1) presented a time-dependent multiterm solution of Boltzmann's equation under nonconservative conditions; (2) acknowledged the existence of the time-dependent hydrodynamic regime and the conditions under which it can be expected to apply; (3) demonstrated the differences which can exist between the bulk and flux transport coefficients and the origin of these differences; (4) demonstrated and interpreted physically the phenomenon of the anomalous negative phase lag, in which the drift velocity preempts changes in the direction of the electric field; and (5) systematically determined the importance of considering the effect of the ejected electron on the temporal profiles of the transport properties undergoing ionization processes. It should be emphasized that the flux and bulk transport properties can vary substantially from one another, and theories which approximate the bulk transport coefficients by the flux transport properties are in general not only wrong in magnitude but also in the phase lags of the temporal profiles. It is only in the very high frequency regime that we have found the bulk and flux transport properties coincide.

The theory and mathematical machinery developed in this work has recently been applied to the space and time modelling of rf parallel plate discharges, incorporating the effects of space-charge through a multiterm solution of Boltzmann's equation for both the electron and ion species in the discharge. This remains the focus of our future investigations.

ACKNOWLEDGMENTS

We wish to thank Professor Zoran Petrovic for his discussions on aspects of this work, and we would like to acknowledge the support of both the Australian Research Council and the High Performance Computing Center at JCU.

APPENDIX: EXISTENCE OF THE HYDRODYNAMIC REGIME

It was acknowledged in Sec. II A that certain assumptions are involved in obtaining the functional form of flux (5) from the assumed functional form of the phase-space distribution function (4). In this section we do not attempt a rigorous proof as to the exact conditions on the validity of the time-dependent hydrodynamic regime, but rather highlight (in the context of the two-term approximation) some of the conditions required in order to validate the flux expansion in Sec.

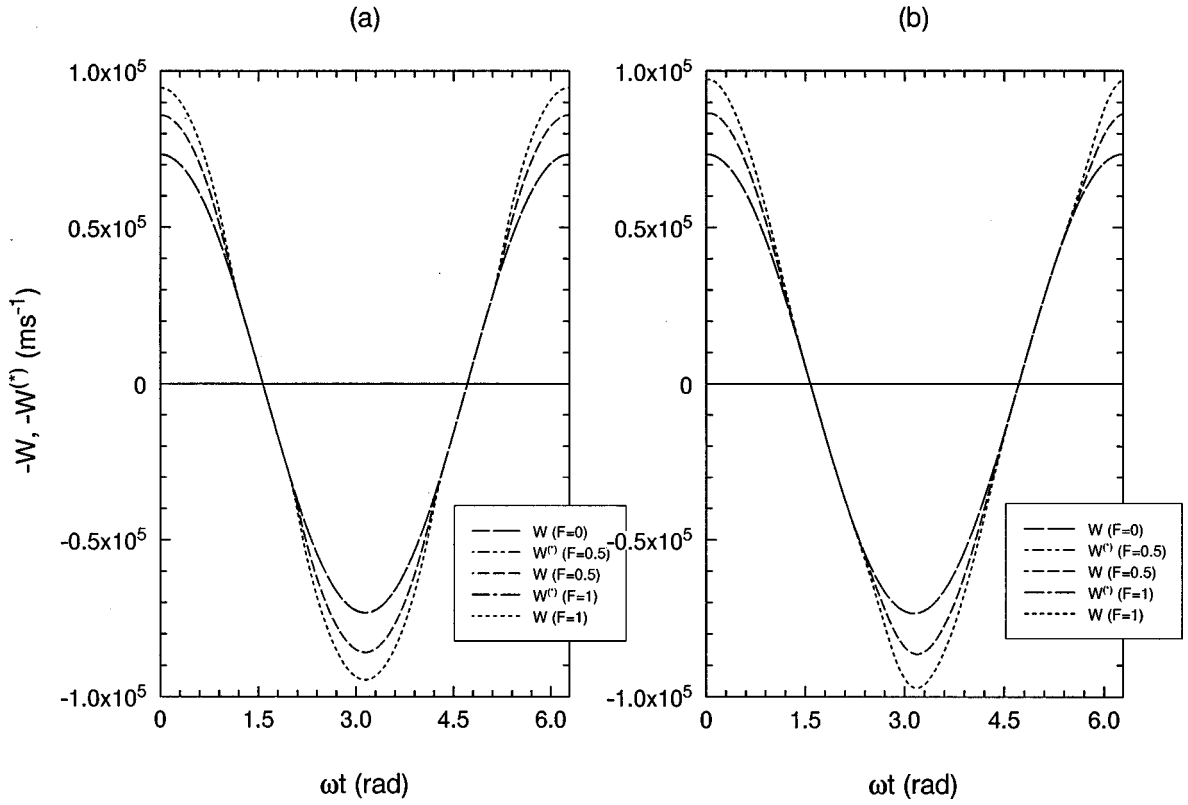

FIG. 10. Temporal variation of the flux and bulk drift velocity for the Lucas-Saelee ionization model (33) for various values of F and applied frequencies ω/n_0 (rad m^3 s^{-1}): (a) 1×10^{-18}; (b) 1×10^{-16}.

II A from the functional form of distribution (4). Other more formal discussions on the transition to a hydrodynamic description in dc electric fields are given in Ref. [43]. The extension to ac electric fields at this stage seem difficult. However, Robson and Makabe [44] investigated the transition to the periodic steady state (where all transients have decayed away, and all properties oscillate at the field frequency or harmonics thereof), using the analytically solvable BGK model.

The starting point is the ''two-term'' approximation of the spherical harmonic representation of the Boltzmann equation (1). For simplicity it is assumed that density gradients are parallel to the field direction, thus maintaining axial symmetry in velocity space. Under such conditions we have

$$\frac{\partial F_0}{\partial t}+\frac{c}{3}\frac{\partial F_1}{\partial z}+\frac{a(t)}{3}\left[\frac{\partial}{\partial c}+\frac{2}{c}\right]F_1=-J^0F_0, \tag{A1}$$

$$\frac{\partial F_1}{\partial t}+c\frac{\partial F_0}{\partial z}+a(t)\frac{\partial F_0}{\partial c}=-J^1F_1=-\nu_mF_1, \tag{A2}$$

where ν_m is the momentum transfer collision frequency and

$$F_l\equiv F_l(z,c,t)=i^l\sqrt{\frac{2l+1}{4\pi}}f_0^{(l)}(z,c,t). \tag{A3}$$

Solution of Eq. (A2) for F_1 yields

$$\begin{aligned}F_1(z,c,t)=F_1(z,c,0)&\exp\left\{-\int_0^t\nu_m[\epsilon(t')dt']\right\}\\&-\int_0^t\exp\left\{-\int_0^\tau\nu_m(\epsilon(t-\tau'))d\tau'\right\}\\&\times\left[c\frac{\partial F_0}{\partial z}(z,c,t-\tau)\right.\\&\left.+a(t-\tau)\frac{\partial F_0}{\partial c}(z,c,t-\tau)\right]d\tau.\end{aligned} \tag{A4}$$

The equivalent of Eq. (4) in terms of the renormalized quantities is

$$F_l(z,c,t)=F_l^{(0)}(c,t)n(z,t)-F_l^{(1)}(c,t)\frac{\partial n}{\partial z}(z,t)+\cdots. \tag{A5}$$

An implicit assumption associated with this particular expansion is that the spatial-dependence is controlled only by the instantaneous number density. (This is a sufficient, but *not* a necessary condition for the existence of the hydrodynamic regime). In what follows we investigate the restrictions implied by this instantaneous density approximation.

Substitution of $l=0$ form of Eq. (A5) into Eq. (A4) yields (to first order in the density gradient)

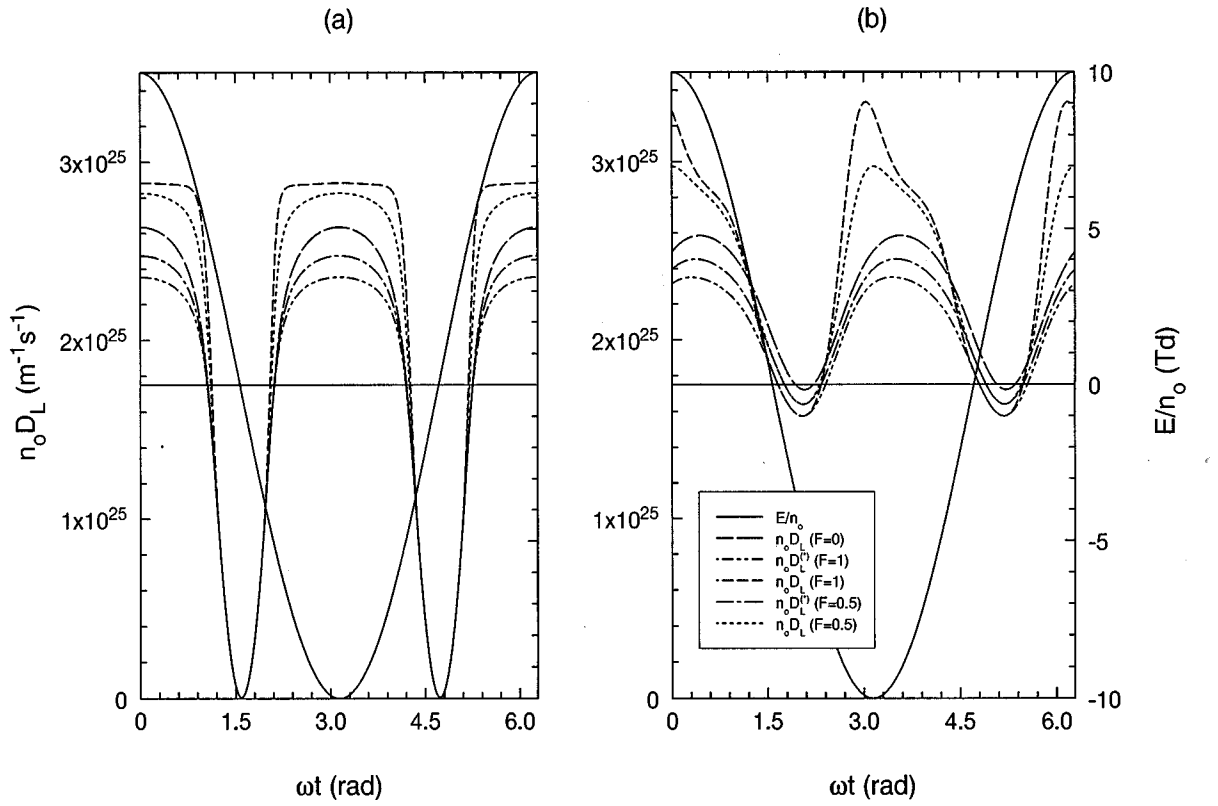

FIG. 11. Temporal variation of the bulk and flux longitudinal diffusion coefficient for the Lucas-Saelee ionization model (33) for various values of F and applied frequencies ω/n_0 (rad m^3 s^{-1}): (a) 1×10^{-18}; (b) 1×10^{-16}. It should be emphasized that the flux and ionization free $F=0$ profiles are essentially the same in this figure.

$$
\begin{aligned}
F_1(z,c,t) = F_1(z,c,0)\exp\left\{-\int_0^t \nu_m(\epsilon(t'))dt'\right\} \\
-\int_0^t \exp\left\{-\int_0^\tau \nu_m(\epsilon(t-\tau'))d\tau'\right\} \\
\times\left\{\left[a(t-\tau)\frac{\partial F_0^{(0)}}{\partial c}(c,t-\tau)\right]n(z,t-\tau)\right. \\
+\left[cF_0^{(0)}(c,t-\tau)+a(t-\tau)\frac{\partial F_0^{(1)}}{\partial c}(c,t-\tau)\right] \\
\left.\times\frac{\partial n}{\partial z}(z,t-\tau)\right\}d\tau. \qquad \text{(A6)}
\end{aligned}
$$

Thus, under a strict nonstationary two-term treatment, we observe that $F_1(z,c,t)$ satisfies a time-dependent hydrodynamic description, i.e., the spatial dependence is described by a linear functional of the number density. We note, however [given a time-dependent density gradient expansion of $F_0(z,c,t)$], that the spatial dependence of $F_1(z,c,t)$ (and hence the charged-particle flux) is *not* a function of the instantaneous number density, and is not directly expressible in the time-dependent density gradient expansion (A5) without additional assumptions. The spatial dependence of $F_1(z,c,t)$ is nonlocal in time. We now investigate the additional assumptions required to reduce Eq. (A6) to the $l=1$ form of the density gradient expansion (A5).

For simplicity we assume a constant collision frequency model (though the arguments are easily extendable to the other models). The first term represents the explicit effects of the initial condition. For times greater than ν_m^{-1}, the effects of initial conditions can be neglected. For $t\gg\tau$,

$$
\begin{aligned}
n(z,t-\tau) = \sum_{j=0}^{\infty}\frac{\tau^j}{j!}\frac{\partial^j n(z,t)}{\partial t^j} \approx n(z,t) \\
\text{if} \quad \tau \ll \left(\frac{1}{n(z,t)}\frac{\partial n(z,t)}{\partial t}\right)^{-1}, \\
\frac{\partial n(z,t-\tau)}{\partial z} = \sum_{j=0}^{\infty}\frac{\tau^j}{j!}\frac{\partial}{\partial z}\left(\frac{\partial^j n(z,t)}{\partial t^j}\right) \approx \frac{\partial n(z,t)}{\partial z} \\
\text{if} \quad \tau \ll \left(\frac{1}{\partial n(z,t)/\partial z}\frac{\partial(\partial n(z,t)/\partial z)}{\partial t}\right)^{-1}.
\end{aligned} \qquad \text{(A7)}
$$

Since the dominant contribution to the integration in Eq. (A6) arises for $\tau\leqslant\nu_m^{-1}$ it follows from Eqs. (A7) that if $n(z,t)$ and its spatial derivatives vary on a time scale less than ν_m^{-1}, i.e.,

$$
\left[\frac{1}{\partial^k n(z,t)/\partial z^k}\frac{\partial}{\partial t}\left(\frac{\partial^k n(z,t)}{\partial z^k}\right)\right]^{-1} \ll \nu_m^{-1}, \qquad \text{(A8)}
$$

a time-dependent density-gradient expansion of $F_1(z,c,t)$ (and thus the charged-particle flux) follows:

$$F_1(z,c,t) = -\int_0^t \exp\left\{-\int_0^\tau \nu_m(\epsilon(t-\tau'))\right\} \times \left[a(t-\tau)\frac{\partial F_0^{(0)}}{\partial c}(c,t-\tau)\right] d\tau\, n(z,t) - \int_0^t \exp\left\{-\int_0^\tau \nu_m(\epsilon(t-\tau'))d\tau'\right\} \times \left[cF_0^{(0)}(c,t-\tau) + a(t-\tau)\frac{\partial F_0^{(1)}}{\partial c} \times (c,t-\tau)\right] d\tau \frac{\partial n}{\partial z}(z,t), \quad \text{(A9)}$$

We are not claiming this to be a rigorous proof as to the conditions required for the existence of the time-dependent hydrodynamic regime, but it serves to highlight that the existence of this regime is dependent solely on the timescales for variation of the number density. We note our arguments to this stage are independent of the form of the applied field. The physical interpretation associated with restrictions (A7) (to first order in the density gradients) are easily understood: (i) the loss rate must be less than the momentum transfer collision frequency; and (2) the distance drifted by the swarm over a time of the order of the momentum relaxation time must be less than the length scale for spatial inhomogeneity. These restrictions can be generalized to higher order coefficients, and are independent of the temporal form of the applied field.

[1] M. A. Liebermann and A. J. Lichtenberg, *Principles of Plasma Discharges and Materials Processing* (Wiley, New York, 1994).

[2] T. Makabe, in *Gaseous Electronics and its Applications*, edited by R. W. Crompton, M. Hayashi, D. E. Boyd, and T. Makabe (KTS Scientific, Tokyo, 1991).

[3] T. Holstein, Phys. Rev. **70**, 367 (1946).

[4] H. Margeneau and L. M. Hartman, Phys. Rev. **73**, 309 (1948).

[5] A. D. MacDonald and S. C. Brown, Phys. Rev. **75**, 411 (1949).

[6] J. Wilhelm and R. J. Winkler, J. Phys. Colloq. **40**, C7–251 (1979); R. Winkler, H. Deutsch, J. Wilhelm, and C. H. Wilke, Beitr. Plasmaphys. **24**, 284 (1984).

[7] D. Loffhagen and R. Winkler, J. Phys. D **29**, 618 (1996); Plasma Sources Sci. Technol. **5**, 710 (1996); D. Loffhagen, G. L. Braglia, and R. Winkler, Contrib. Plasma Phys. **38**, 527 (1998).

[8] T. Makabe and N. Goto, J. Phys. D **21**, 887 (1988); N. Goto and T. Makabe, *ibid.* **23**, 686 (1990).

[9] K. Maeda and T. Makabe, Jpn. J. Appl. Phys. Part 1 **33**, 4173 (1994); Phys. Scr. **T53**, 61 (1994).

[10] K. Maeda, T. Makabe, N. Nakano, S. Bzenic, and Z. Lj. Petrovic, Phys. Rev. E **55**, 5901 (1997).

[11] C. M. Ferreira, L. L. Alves, M. Pinheiro, and A. B. Sa, IEEE Trans. Plasma Sci. **19**, 229 (1991); C. M. Ferreira and J. Loureiro, J. Phys. D **17**, 1175 (1984); *ibid.*, **22**, 76 (1989).

[12] J. Loureiro, Phys. Rev. E **47**, 1262 (1993).

[13] U. Kortshagen, Plasma Sources Sci. Technol. **26**, 1230 (1993); **4**, 172 (1995).

[14] Z. Lj. Petrovic, J. V. Jovanovic, Z. M. Raspopovic, S. A. Bzenic, and S. B. Vrhovac, Aust. J. Phys. **50**, 591 (1997); S. Bzenic, Z. M. Raspopovic, S. Sakadvic, and Z. Lj. Petrovic, IEEE Trans. Plasma Sci. **27**, 78 (1999); S. Bzenic, Z. Lj. Petrovic, Z. M. Raspopovic, and T. Makabe, Jpn. J. Appl. Phys. (to be published); Z. Lj. Petrovic, S. Bzenic, and T. Makabe, in *Proceedings of the International Symposium on Electron-Molecule Collisions and Ion and Electron Swarms*, edited by M. Allen (Institute of Physical Chemistry, University of Fribourg, Fribourg, 1997),

[15] R. E. Robson, K. Maeda, T. Makabe, and R. D. White, Aust. J. Phys. **48**, 335 (1995).

[16] R. D. White, R. E. Robson, and K. F. Ness, Aust. J. Phys. **48**, 925 (1995).

[17] R. E. Robson, R. D. White, and T. Makabe, Ann. Phys. (Leipzig) **261**, 74 (1997).

[18] R. D. White, R. E. Robson, and K. F. Ness, J. Vac. Sci. Technol. A **16**, 316 (1998).

[19] R. E. Robson, Aust. J. Phys. **50**, 577 (1991).

[20] W. L. Morgan and B. M. Penetrante, Comput. Phys. Commun. **58**, 127 (1990).

[21] R. E. Robson and K. F. Ness, Phys. Rev. A **33**, 2068 (1986).

[22] K. F. Ness and R. E. Robson, Phys. Rev. A **34**, 2185 (1986).

[23] K. Kumar, H. R. Skullerud, and R. E. Robson, Aust. J. Phys. **86**, 845 (1980).

[24] K. Kumar, J. Phys. D **14**, 2199 (1981).

[25] S. Chapman and T. G. Cowling, *The Mathematical Theory of Non-uniform Gases* (Cambridge University Press, Cambridge, England, 1936).

[26] K. Kumar and R. E. Robson, Aust. J. Phys. **26**, 157 (1973).

[27] P. Waltman, *A Second Course in Elementary Differential Equations* (Academic, Orlando, FL, 1986).

[28] R. D. White, K. F. Ness, R. E. Robson, and B. Li, Phys. Rev. E **60**, 2231 (1999).

[29] L. Boltzmann, Wein. Ber. **66**, 275 (1872).

[30] C. S. Wang-Chang, G. E. Uhlenbeck, and J. De Boer, in *Studies in Statistical Mechanics*, edited by J. De Boer and G. E. Uhlenbeck (Wiley, New York, 1964), Vol. II, p. 241.

[31] K. Kumar, Ann. Phys. (Leipzig) **37**, 113 (1967).

[32] K. Ness and R. E. Robson, Transp. Theory Stat. Phys. **14**, 257 (1985).

[33] R. D. White, Ph.D. thesis, James Cook University, Cairns, Australia, 1996.

[34] H. R. Skullerud, J. Phys. B **2**, 696 (1969).

[35] H. Sugawara, Y. Sakai, and S. Sakamoto, J. Phys. D **30**, 368 (1997).

[36] A. M. Nolan, M. J. Brennan, K. F. Ness, and A. B. Wedding, J. Phys. D **30**, 2865 (1997).

[37] B. Li, R. E. Robson, and R. D. White (unpublished).

[38] J. Lucas and H. Saelee, J. Phys. D **8**, 640 (1975).

[39] T. Tanaguchi, H. Tagashira, and Y. Sakai, J. Phys. D **10**, 2301 (1977).

[40] Z. Raspopovic, S. Sakadvic, Z. Lj. Petrovic, and T. Makabe (unpublished).

[41] Z. Raspopovic, S. Sakadvic, S. Bzenic, and Z. Lj. Petrovic,

IEEE Trans. Plasma Sci. (to be published); S. Sakadvic, Z. Lj. Petrovic, Z. Raspopovic, and N. Petrovic, in *Proceedings of the International Symposium on Electron-Molecule Collisions and Swarms* (*a Satellite of XXI ICPEAC*), edited by Y. Hatano, T. Tanaka, and K. Kouchi (Department of Chemistry, Tokyo Institute of Technology, Tokyo, 1999), p. 115.

[42] R. E. Robson and R. D. White (unpublished).

[43] K. Kumar, J. Phys. D **14**, 2199 (1981); Aust. J. Phys. **48**, 365 (1995); **40**, 367 (1987).

[44] R. E. Robson and T. Makabe, Aust. J. Phys. **47**, 305 (1994).